Sensitivity and Correlation Analysis of PROSPECT-D and ABM-B Leaf Models

Reisha D. Peters and Scott D. Noble

***Abstract*— Two leaf optical property models, PROSPECT-D and ABM-B, were compared to determine their respective parameter sensitivities and to correlate their parameters. ABM-B was used to generate 150 leaf spectra with various input parameters, and the inversion of PROSPECT-D was used to estimate leaf parameters from these spectra. Wavelength-specific sensitivities were described, and correlations were developed between the leaf pigments and structure parameters of the two models. Of particular importance was the correlation of PROSPECT-D's structure parameter (*N*) which is a generalized parameter integrating several leaf-level and cell-level characteristics. At the leaf-level, *N* showed correlations with the leaf thickness and the mesophyll percentage, and at the cell-level, *N* was affected by the cell cap aspect ratios defined in ABM-B. The estimated value of *N* also varied substantially with changes in the angle of incidence specified in ABM-B. All of these correlations were nonlinear, and it is unclear how these parameters are combined to affect the final value for *N*. The correlations developed in this article indicate that additional structural parameters (possibly separated into leaf-level and cell-level) should be considered in future model development that aims to maintain inversion potential while providing more information about the leaf.**

***Index Terms*— ABM, leaf pigment absorption, mathematical leaf modeling, PROSPECT, reflectance, sensitivity, spectroscopy, transmittance.**

I. Introduction

THE reflectance (R) and transmittance (T) spectra of plant leaves are affected by many factors related to the plant species, the environment, and the biochemical and biophysical attributes of the plant. Surface characteristics, water concentration, leaf thickness, pigment concentration, and disease can all affect the way a plant leaf interacts with light. Light reflectance and transmittance spectra at the surface of plant leaves can be indicative of the biochemical attributes of plants and can be exploited as a nondestructive method for their estimation. Currently, there are leaf models that can estimate some of these biochemical and biophysical attributes through model inversion, but they have limitations. Hemispherical reflectance and transmittance measurements are often used in leaf modeling, but away from a laboratory setting, collecting these measurements is not always practical. Leaf data sets that are widely used in model calibration, such as LOPEX and ANGERS [1], [2], are biased toward healthy, green tree leaves. This can result in good modeling results for similar plants, but may not extend to varieties or traits not represented in the calibration data. Models also tend to group highly correlated parameters, such as chlorophyll a and b, or use generalized structural features. This does not present an issue for species which follow a standard correlation trend, but for atypical leaves some information may be missed. Although these limitations exist, leaf models are routinely used in field settings. To increase the amount of data that can be collected from plant spectral measurements an expanded model is necessary. This model should maintain invertibility while accounting for additional leaf features (including leaf angle as in PROCOSINE [3] and surface features) and additional (or more narrowly specified) pigments. Differentiating between C3 and C4 plants may also be required [4], [5]. A first step to this end is to examine current leaf models and perform and sensitivity and correlation analysis between them to determine their respective capabilities. The work presented in this article investigates and compares PROSPECT-D [6] and ABM-B [7].

Modeling biochemical properties of leaves from reflectance and transmittance measurements at the leaf surface has been a developing field in the remote sensing community for nearly 50 years with some of the earliest work relating leaf structure and reflectance [8]. Major advancements in this field have seen the development of several models that can generate leaf spectra based on measured biochemical and biophysical properties of leaves [7], [9], [10]. Perhaps, the most well-known and widely used model is PROSPECT, originally developed by Jacquemoud and Baret [10] and further expanded by many other researchers [6], [10]. PROSPECT has not only been used for modeling spectra but can also be inverted to estimate leaf biochemical and biophysical properties given the reflectance and transmittance spectra of a leaf [6], [11].

The original PROSPECT model used equivalent water thickness, chlorophyll concentration, and a leaf structure parameter to model leaf reflectance and transmittance [10]. Advancements to the model have seen the addition of dry matter, carotenoids, and brown pigments [2], and most recently the anthocyanins [6]. With the addition of each pigment, specific absorption coefficients (SACs) were recalibrated and the refractive index characterization was enhanced. PROSPECT-D uses a generalized plate model approach [12]. A variation of the Beer-Lambert Law with specific absorption coefficients and area-based concentrations is used to approximate the absorption of a single layer of leaf material. Refraction is

Manuscript received March 11, 2019; revised June 11, 2019, November 14, 2019, and February 21, 2020; accepted March 19, 2020. Date of publication April 28, 2020; date of current version November 24, 2020. This work was supported in part by the Plant Phenotyping and Imaging Research Centre funded through the Canada First Research Excellence Fund (CFREF). *(Corresponding author: Reisha D. Peters.)*

Reisha D. Peters is with the Department of Chemical and Biological Engineering, University of Saskatchewan, Saskatoon, SK S7N 5A9, Canada (e-mail: reisha.peters@usask.ca).

Scott D. Noble is with the Department of Mechanical Engineering, University of Saskatchewan, Saskatoon, SK S7N 5A9, Canada (e-mail: scott.noble@usask.ca).

Color versions of one or more of the figures in this article are available online at https://ieeexplore.ieee.org.

Digital Object Identifier 10.1109/TGRS.2020.2983856

simulated at the bounds of each leaf layer as well as at the upper and lower surfaces of the leaf.

The algorithmic bidirectional scattering distribution function model for bifacial plant leaves (ABM-B) works from a first principles approach and requires more input variables to generate the reflectance and transmittance spectra of leaves. This model simulates leaf-light interaction using an algorithmic Monte Carlo method [7]. ABM-B aims to recreate the interactions between an individual ray and the leaf tissue and combines the results from a user-specified number of iterations. Biophysical properties such as leaf structure and cellular roughness are described by thickness and cell cap aspect ratios, respectively. ABM-B also includes a sieve effect parameter which considers the possibility of light traveling through the medium without encountering an absorbing component [13]. This model relies on stochastic methods of spectra generation and requires more input parameters making inversion time consuming and computationally expensive. However, the increased number of biophysical parameters has the potential to provide more information about the effects of specific physical characteristics. Unlike the PROSPECT-D model, many input parameters of ABM-B are specified in volume-based concentrations. Therefore, a combination of parameters such as thickness (t) and mesophyll percentage (m) in ABM-B will be required to compare pigment quantities. ABM-B also has a constant volumetric concentration for water and the water path length is adjusted with the leaf thickness.

One key difference between ABM-B and PROSPECT-D is in the underlying specific absorption coefficients used in the models. PROSPECT-D uses separate SACs for chlorophyll, carotenoids, and anthocyanins. However, ABM-B uses the chlorophyll SAC based on an earlier version of PROSPECT [14] that effectively treated all pigments as chlorophyll [2] and would have included some carotenoid and anthocyanin absorption when calibrating the "chlorophyll" SAC.

A direct comparison between ABM-B and PROSPECT-D has not been published previously, but there is substantial work done on comparisons between other leaf models at both the canopy and leaf levels [15], [16].

The PROSPECT model allows for inversion (obtaining leaf parameters from input spectra) but some of the parameters represent a series of integrated leaf parameters and are difficult to link to measurable attributes. The ABM-B model has a larger number of user inputs, but is difficult to invert. The PROSPECT model has also been validated through testing from multiple researchers [2], [3], [6], [11], whereas ABM has been less prominent in the remote sensing community, possibly due to the lack of a current invertible version.

The objective of comparing these models is to interrogate the generalized parameters of PROSPECT-D using the more specific parameters of ABM-B. By better understanding these relationships, candidate modifications to how PROSPECT handles structure may become evident. Additionally, the most significant parameters may be targeted for measurements and inclusion in expanded training data sets. For this purpose, only simulated spectra were used; no observations from real leaf specimens were used. This allows for input parameters that are fully specified as opposed to underlying biophysical characteristics are difficult to know with certainty. By extension, comparisons of the models' absolute accuracy in reconstructing spectra are not explored.

TABLE I
MAXIMUM AND MINIMUM VALUES FOR PARAMETERS USED TO GENERATE SPECTRA WITH THE ABM-B AND PROSPECT-D LEAF MODELS

	Parameters (units)		
	ABM-B Parameters		
	Number of Samples	100000	
	Wavelength Range (nm)	400-2500	
	Surface of incidence	Adaxial	
Name		Minimum	Maximum
t	Leaf thickness (mm)	0.070	0.300
m	Mesophyll percentage (%)	2.68	93.16
C_{chla}	Chlorophyll A concentration (g/cm^3)	0.00020	0.00627
C_{chlb}	Chlorophyll B concentration (g/cm^3)	0.00011	0.00233
C_{car}	Carotenoid concentration (g/cm^3)	0.00010	0.00229
C_{pro}	Protein concentration (g/cm^3)	0.01442	0.18000
C_{cel}	Cellulose concentration (g/cm^3)	0.00202	0.21013
C_{lig}	Lignin concentration (g/cm^3)	0.00081	0.11296
δ_c	Cuticle undulations aspect ratio	1	25
δ_e	Epidermis cell caps aspect ratio	1	25
δ_p	Palisade cell caps aspect ratio	1	25
δ_s	Spongy cell caps aspect ratio	1	25
sieve	Simulate sieve effects	No	Yes
θ	Angle of incidence (degrees)	0	45
	PROSPECT-D Parameters		
N	N	1	3
C_{ab}	Chlorophyll A+B (μg/cm^2)	0.7	100
C_{xc}	Carotenoids (μg/cm^2)	0.05	30
C_{anth}	Anthocyanins (μg/cm^2)	0	3
C_{br}	Brown Pigments (arbitrary units)	0	1
C_w	Water (cm)	0.00057	0.06000
C_m	Dry Matter (g/cm^2)	0.00024	0.03000

II. METHODS

One hundred and fifty sets of leaf parameters were used to generate leaf spectra using ABM-B. The inverse mode of PROSPECT-D was then used to estimate the set of PROSPECT-D input parameters that would best match the spectra generated using ABM-B. Table I lists the full set of input parameters for each model, their units, the symbols used in the text to refer to them, and the bounds placed on them. These minimum and maximum values were determined based on the values collected in the LOPEX database [1]. For PROSPECT-D, these values could be directly interpreted from the data set, but for ABM-B, some parameter maxima and minima had to be calculated. In ABM-B, pigment concentrations are specified on a per-volume basis. To approximate maximal and minimal values for these parameters, the per-area based concentrations from LOPEX were divided by the leaf thickness. The maximum values for the cell cap aspect ratio parameters were set to 25 which is half of the allowable value in the online ABM-B model. The 150 sets of parameters included both specifically chosen values and randomly generated combinations of values within the bounds specified in Table I. Within these parameter sets, 79 used standard values for the epidermis cell cap aspect ratio ($\delta_e = 5$), palisade cell cap aspect ratio ($\delta_p = 1$), spongy cell cap aspect ratio ($\delta_s = 5$), cuticle undulation aspect ratio ($\delta_c = 1$), and angle of incidence

($\theta = 0$), and included sieve effects according to the default values in ABM-B (as estimated for a soybean leaf). These parameter sets will be referred to as cell cap ratio constant ($CCR_{constant}$). The other 71 sets included changes to all or some of these parameters in addition to others and will be referred to as $CCR_{varying}$. The use of the standard values in a portion of the parameter sets allowed for separate evaluation of the effects of the structural parameters in the ABM-B model.

In its current online form [17], ABM-B generates spectra that have 5-nm wavelength intervals. Linear interpolation was used to adjust these spectra to the 1-nm intervals used in PROSPECT-D. The total reflectance (specular plus diffuse) and the transmittance from ABM-B were used as the inputs for the PROSPECT-D inversion. PROSPECT-D was used to estimate leaf parameters using the inversion method outlined in the PROSPECT-4 and 5 article [2]. This method uses a numerical inversion and a constrained Powell's search method. Three initial starting points were used for the search to investigate the equifinality associated with the model and two additional inversions were performed to exclude the brown pigments (C_{br}) and both anthocyanins (C_{anth}) and brown pigments as these pigments are not explicitly included in the ABM-B model.

In addition to spectra generated by ABM-B, a set of spectra was generated by using PROSPECT-D in the forward direction to investigate the sensitivity of PROSPECT-D to its input parameters. The parameters for these spectra were chosen within the bounds described in Table I.

The spectra generated by ABM-B and PROSPECT-D and the parameters of each model were examined in three stages. First, the wavelength-specific sensitivities of each model to their respective parameters were calculated. Second, the output spectra from ABM-B and inverted spectra from PROSPECT-D were compared (for selected sets of parameters). Finally, correlations were shown for each parameter in the PROSPECT-D model in relation to the ABM-B parameters.

Wavelength-specific spectral sensitivities were calculated using a simple linear regression between each parameter and the reflectance (or transmittance) for every wavelength individually. The slope of the linear regression (%R or %T per parameter unit value) was used to approximate the effect of the parameter on the absorptance [18]. This method provides a quick qualitative comparison of the effects of each parameter but can be affected by parameter saturation effects. To assess these possible saturation effects, coefficients of determination were also calculated for the regression lines. These results are summarized in Section III.

The spectra generated by ABM-B were compared to those fit in the PROSPECT-D inversion for four individual parameter sets. This comparison was used to hypothesize how the effects of specific structural parameters affect PROSPECT-D's ability to model the spectra. All inversions were used in these examples, and the results are summarized in Section IV.

Although many input parameters (e.g., pigment concentrations) have similar meanings in ABM-B and PROSPECT-D, few are reported with the same units. To allow for a direct comparison of the pigments, water content, and dry matter, parameters used in the ABM-B model were combined resulting in compatible units between the models. The per-volume pigment and dry matter concentrations from ABM-B were multiplied by the thickness, mesophyll percentage, and a necessary unit conversion for each sample to obtain per-area concentration values. The water content in ABM-B was determined by multiplying the leaf thickness with the percentage of leaf thickness occupied by the mesophyll tissue (mesophyll percentage). This was directly compared to the water content in PROSPECT-D which is described as an equivalent water thickness (C_w) with units of centimeters. The correlations between the seven parameters described in PROSPECT-D and those specified in ABM-B are summarized in Section V.

III. Wavelength-Specific Sensitivities

The sensitivities for each parameter in ABM-B are shown in Fig. 1 with a 20-nm wide moving average applied to reduce the noise associated with the stochastic nature of the model. The coefficients of determination that were calculated for each regression line were above 0.6 for all wavelengths shown in Fig. 1 except for parameters which had very little effect on the reflectance spectra such as protein (C_{pro}), cellulose and lignin ($C_{cel+lig}$), δ_c, and δ_s. Although the coefficients of determination are high, these results are dependent on the limited data set used in this analysis and cannot be considered as absolute for all data sets. Fig. 1(a)–(d) shows the effect that each parameter has on reflectance and Fig. 1(e)–(h) shows the effect on transmittance. The sensitivities of chlorophyll a and b (C_{chla+b}) and carotenoids (C_{car}) approach 0 above 800 nm as they do not affect the NIR portion of the spectra so only the 400–800 nm range is shown for these pigments. The shape of these two sensitivity spectra follows a similar shape to the absorption spectra of these two pigments. This is expected as the reflectance is affected by how much light the leaf absorbs and should show an inverted version of the pigment absorption spectra. Increasing C_{chla+b}, C_{car}, t, m, C_{pro}, and $C_{cel+lig}$ cause a decrease in the estimated reflectance and transmittance of a leaf. θ, shown in Fig. 1(b) and (f), causes an increase in reflectance and decrease in transmittance. The sieve parameter will also cause an increase in reflectance due to the reduced probability of light absorption [19]. The δ_p, δ_e, and δ_s cause decreases in reflectance, but also induce an increase in transmittance that is similar in magnitude to the reflectance decrease.

The sensitivity spectra for the PROSPECT-D parameters are shown in Fig. 2. C_{ab}, C_{xc}, C_{anth}, C_w, C_m, and C_{br} cause a decrease in reflectance and transmittance when their values are raised. The N parameter causes an increase in reflectance, but decrease in transmittance as its value increases. The N parameter accounts for multiple leaf features, but if it is considered to capture the leaf thickness as part of its function then this result is expected. The sensitivity spectra for PROSPECT-D chlorophyll (C_{ab}), carotenoids (C_{xc}), and C_{anth} are similar in shape to the absorption spectra for these pigments and are shown in the 400–800 nm range to highlight their region of influence. These pigments have a similar effect on reflectance and transmittance as they increase the

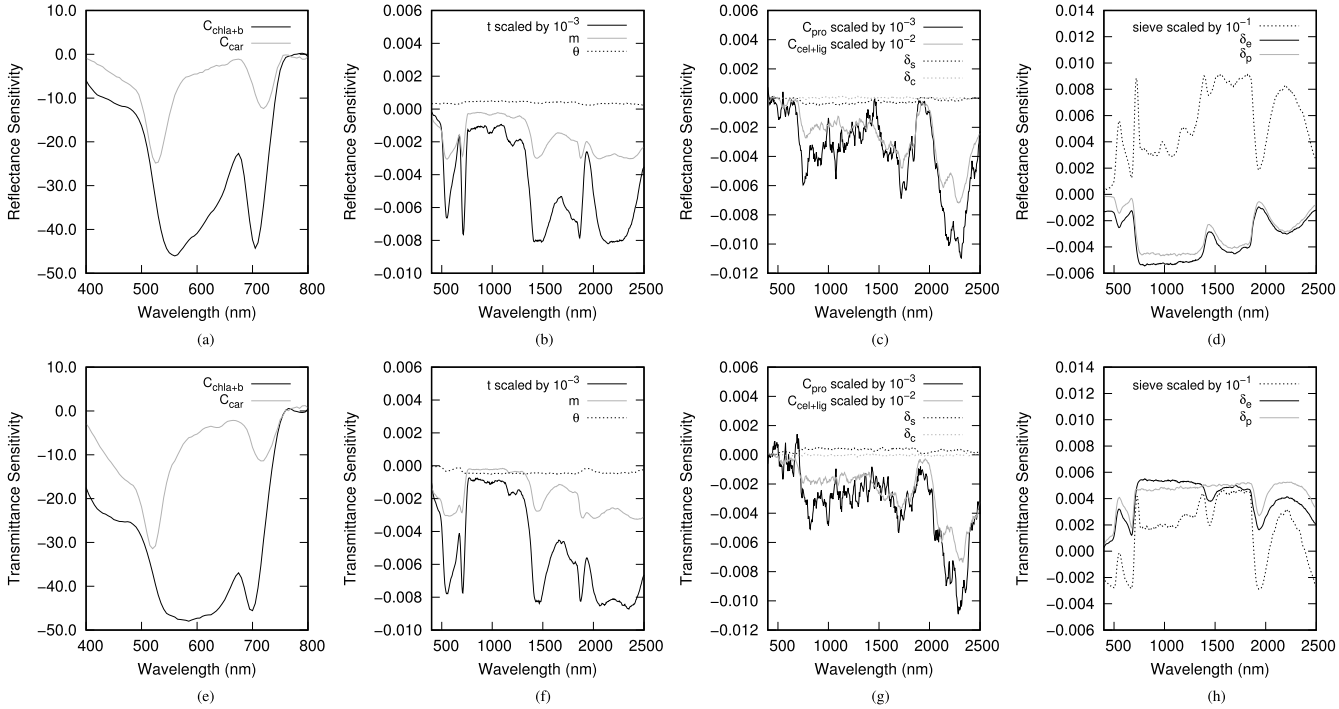

Fig. 1. Wavelength-specific sensitivities to the input parameters in ABM-B, with scaling factors for graphing purposes indicated. (a) Reflectance sensitivity to $C_{\text{chla+b}}$ and C_{car}. (b) Reflectance sensitivity to t, m, and θ. (c) Reflectance sensitivity to C_{pro}, $C_{\text{cel+lig}}$, δ_{s}, and δ_{c}. (d) Reflectance sensitivity to δ_{e}, δ_{p}, and sieve. (e) Transmittance sensitivity to $C_{\text{chla+b}}$ and C_{car}. (f) Transmittance sensitivity to t, m, and θ. (g) Transmittance sensitivity to C_{pro}, $C_{\text{cel+lig}}$, δ_{s}, and δ_{c}. (h) Transmittance sensitivity to δ_{e}, δ_{p}, and sieve.

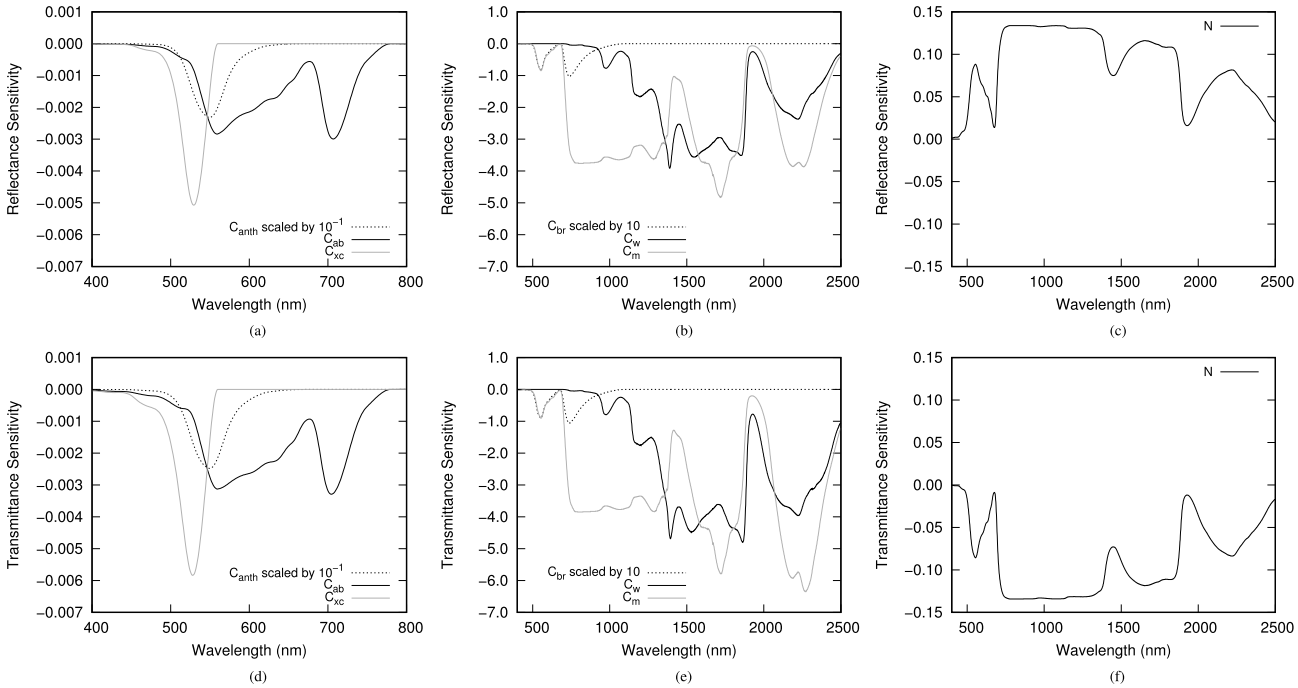

Fig. 2. Wavelength-specific sensitivities to the input parameters in PROSPECT-D. (a) Reflectance sensitivity to C_{ab}, C_{xc}, and C_{anth}. (b) Reflectance sensitivity to C_{w}, C_{m}, and C_{br}. (c) Reflectance sensitivity to N. (d) Transmittance sensitivity to C_{ab}, C_{xc}, and C_{anth}. (e) Transmittance sensitivity to C_{w}, C_{m}, and C_{br}. (f) Transmittance sensitivity to N.

light that is absorbed by the leaf. As expected, a correlation between the spectral shapes of the C_{ab} sensitivity and the $C_{\text{chla+b}}$ sensitivity, as well as the C_{car} and C_{xc} sensitivities can be seen. Although these two models use different specific absorption coefficients, the general shape of these coefficients is very similar. The dry matter (C_{m}) sensitivity spectrum presents some similarities to the C_{pro} and $C_{\text{cel+lig}}$ sensitivity spectra from the ABM-B model. It is not immediately clear which parameters from ABM-B correlate best with the N and C_{w} parameters in PROSPECT-D and there are likely some combinations of ABM parameters that best describe these PROSPECT-D parameters. The C_{br} sensitivity spectrum is

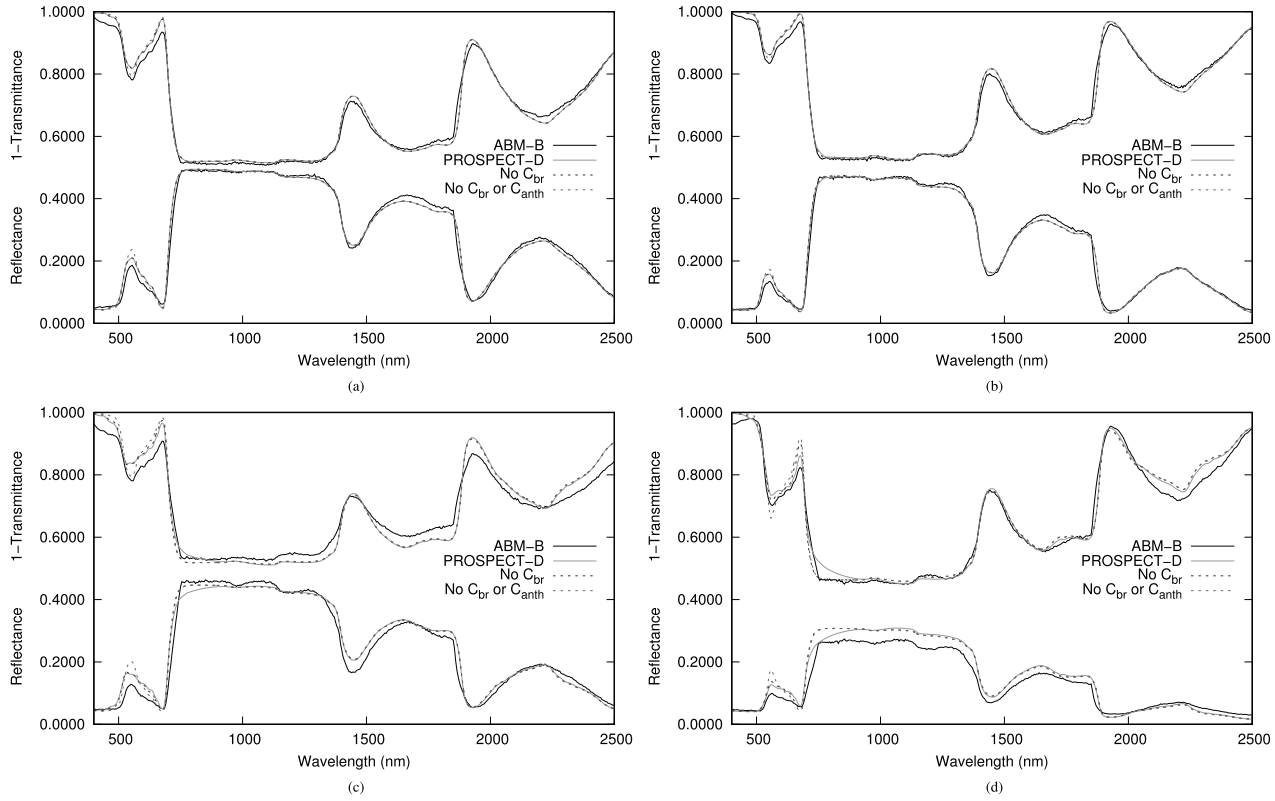

Fig. 3. Four sets of spectra modeled by ABM-B and PROSPECT-D using the parameters as listed in Table II. Reflectance and 1—Transmittance are shown. Plots (a)—(c) use the same cellular aspect ratios. Plot (b) displays changes in pigment values and leaf-level structure parameters and (c) uses the same parameters as (a) but does not include ABM-B's sieve effects. Plot (d) has a completely different set of parameters from (a) and does not account for sieve effects. Plot (d) represents a spectrum that should be difficult to invert in PROSPECT-D due in part to the nonnadir illumination.

unlike any of the spectra seen in the ABM-B sensitivities. This pigment is not well defined in any of the PROSPECT models, but appears to be similar to some "decay pigments" and may be useful for monitoring aging leaves [20]. In previous models, the brown pigments have been described as polyphenols that appear during the drying process [21], [22] or more specifically tannins for which there were no current methods for determining concentration [10]. Recent work has studied the effects of including and excluding brown pigments in multiple inversions of the PROSPECT model. One study found that the pigment estimations for chlorophyll and carotenoids were improved when brown pigments were included in the model [11]. Due to the unclear nature of these brown pigments in the model, results with and without their inclusion will be presented.

IV. Comparison of ABM-B Spectra and PROSPECT-D Spectra Fit in Inversion

A direct comparison of spectra generated by ABM-B and those fit through the inversion of PROSPECT-D highlights the differences and similarities between the models and identifies where model advancements may be possible. Fig. 3 shows four sets of transmittance and reflectance spectra that were generated by ABM-B as well as the spectra from PROSPECT-D that were fit during inversion. In these examples, a single set of ABM-B spectra (reflectance and transmittance) is shown for each sample and three PROSPECT-D inversion spectra sets are shown. These three PROSPECT-D spectra represent the cases with all pigments included, without C_{br}, and without C_{br} or C_{anth}. In addition to these cases, two alternate initial conditions with all pigments included were investigated in the inversion, but there was no statistically significant difference in the spectral or parameter estimation results (ANOVA returned a p-value of 0.99). Although this does not negate the potential for equifinality in the inversion, it provides evidence that the initial condition does not strongly affect the inversion in the data presented in this work. Input parameters to ABM-B and resulting PROSPECT-D parameters (including C_{anth} and C_{br}) estimated based on the ABM-B spectra are summarized in Table II. Fig. 3(a) shows the ABM-B spectra generated with parameter values typical for an average leaf (as determined in the LOPEX database) and the corresponding spectra fit through PROSPECT-D inversion. The reflectance and transmittance spectra fit by PROSPECT-D are very similar to the ABM-B spectra in this example. In the case of anthocyanin being excluded from PROSPECT-D, there is a more pronounced peak near 550 nm (this reflectance increase near 550 nm is visible in all four samples shown in this figure). This highlights the differences between the SACs used in each model as discussed in Section I where the chlorophyll SAC in ABM-B is incorporating the carotenoid and anthocyanin SACs. The PROSPECT-D chlorophyll SAC is consequently lower than the ABM-B SAC in the 550-nm region. The average root mean square error (RMSE) values for these spectra are 0.0143 for R and 0.0164 for T. Fig. 3(b) represents another set of parameters that has different

TABLE II
TABLE OF VALUES FOR FIG. 3 PARAMETERS FOR FOUR OF THE 150 CASES ARE SHOWN

Parameters	Sample 1 (A)	Sample 41 (B)	Sample 113 (C)	Sample 122 (D)
ABM-B – Input Parameters				
t (mm)	0.112	0.215	0.112	0.241
m (%)	50.00	17.78	50.00	68.42
C_{chla} (g/cm^3)	0.002956	0.005296	0.002956	0.000236
C_{chlb} (g/cm^3)	0.001032	0.000321	0.001032	0.000794
C_{car} (g/cm^3)	0.000566	0.000515	0.000566	0.002106
C_{pro} (g/cm^3)	0.08132	0.095302	0.08132	0.14106
C_{cel} (g/cm^3)	0.03597	0.069517	0.03597	0.07415
C_{lig} (g/cm^3)	0.00671	0.015427	0.00671	0.10322
δ_c	1	1	1	11
δ_e	5	5	5	19
δ_p	1	1	1	4
δ_s	5	5	5	11
sieve	yes	yes	no	no
θ (degrees)	0	0	0	27
PROSPECT-D Parameters from inversion of spectra generated by ABM-B				
N	1.63989	1.60354	1.48975	1.00000
C_{ab} (μg/cm^2)	21.1646	32.6391	18.2597	8.50119
C_{xc} (μg/cm^2)	5.69637	7.80605	2.66794	11.4925
C_{anth} (μg/cm^2)	1.17304	0.96987	1.39678	0.00014
C_{br} (a.u.)	0.00007	0.05658	0.28508	0.55809
C_w (cm)	0.00643	0.01184	0.00714	0.01137
C_m (g/cm^2)	0.00259	0.00577	0.00716	0.01660

values for the leaf biochemistry, thickness, and mesophyll but the same cellular aspect ratio values and illumination angle. Again, PROSPECT-D is able to match the spectra effectively. The overall fit between these spectra is high with average RMSE values of 0.0115 for R and 0.0137 for T.

In both Fig. 3(a) and (b), PROSPECT-D estimates a slightly lower reflectance in portions of the NIR and a higher reflectance in portions of the visible. The opposite is true for transmittance; PROSPECT-D estimates lower transmittance in the visible region and higher in portions of the NIR. The combination of reflectance and transmittance deviations may indicate the estimated value of N is a compromise. Other differences between the two models that may be contributing to the inability to achieve a good match in the full spectra are the shapes of the SACs, as discussed previously, and the refractive indices. For refractive index, PROSPECT-D uses a single spectrum for the whole leaf, but ABM-B uses different spectra for the epicuticular wax and the mesophyll cell walls. These refractive index spectra are also different in shape. The spectrum from PROSPECT-D [6] has a more pronounced decrease in refractive index with increasing wavelength compared to any of the ABM-B refractive index spectra [7].

Fig. 3(c) uses the same parameters as (a) but does not account for sieve effects. A major difference between these two spectra is the increase in the amount of transmittance and the decrease in reflectance across the whole wavelength range. The spectra estimated by PROSPECT-D are not as similar to the generated spectra and have an RMSE value of 0.0247 for R and 0.0327 for T in this sample. Differences are observed in the 400–800 nm range where the reflectance is much higher in the PROSPECT-D spectra than ABM-B. Additionally, the reflectance between 800 and 1000 nm is lower in the spectra estimated by PROSPECT-D. A shape contrast is also present in this region at the red edge; ABM-B has a sharp decrease in reflectance and transmittance, whereas the decrease is more gradual in the PROSPECT-D model. In the inversion case where brown pigments are included, the rounded red-edge is more prominent. It should be noted that neither model is portraying an accurate spectral feature for leaves at the red-edge and a typical leaf spectrum would lie somewhere between these two extremes [1], [2]. The PROSPECT-D transmittance is lower in the 400–800 nm range and higher between 1500 and 2000 nm compared to the ABM-B spectra. Comparing Fig. 3(a) to 3(c), there is less reflectance in (c) and a wider gap in the NIR plateau between reflectance and transmittance. The decrease in reflectance is a result of increased absorption in the absence of sieve effects. The parameter estimations from PROSPECT-D as summarized in Table II indicate how PROSPECT-D is accounting for this suppression of sieve effects. The N parameter is decreased to account for the lower reflectance in Fig. 3(c). In the PROSPECT-D model, N represents the number of homogeneous layers separated by air spaces within the leaf [10]. As N decreases, the number of interfaces for potential reflectance also decreases resulting in less reflectance and more transmittance through the leaf. C_{br} is increased from (a) to (c). This increase in brown pigment is common to all spectra generated without the use of sieve effects.

Fig. 3(d) uses different biochemical, leaf thickness, and mesophyll values than (a) as well as different cellular aspect ratios, and angle of incidence. This sample also does not account for sieve effects in the ABM-B model. These spectra have RMSE values of 0.0282 for R and 0.0233 for T. PROSPECT-D estimates higher reflectance and lower transmittance for most wavelengths in these spectra. This is a result of the N parameter reaching the bounded lower limit of 1 in the inversion; the reflectance cannot be further reduced in PROSPECT-D by altering N. The PROSPECT-D reflectance also has more subtle water absorption bands near 900 and 1200 nm. The rounded red-edge due to brown pigment inclusion is visible in these spectra as well, and although their exclusion improves the shape match between ABM-B and PROSPECT-D spectra, the offset between the spectra is increased. These results are not surprising as PROSPECT-D assumes a hemispherical (or equivalent) measurement and a set angle of illumination and does not directly account surface changes in cell cap aspect ratios. This inversion example also has a high estimation for C_{br} (Table II).

The only parameter in PROSPECT-D that can account for all of the changes in the cellular aspect ratios is the N parameter. However, N is also affected by the mesophyll characteristics and thickness of the leaf among other physical parameters. Inverting spectra that are generated with large incident angles (to the normal) are out of the scope of the design of PROSPECT-D. However, their inclusion in future invertible models will improve parameter estimation and model robustness.

V. CORRELATION BETWEEN PROSPECT-D AND ABM-B PARAMETERS

PROSPECT-D has seven parameters that are used to model leaf reflectance and transmittance spectra. In the

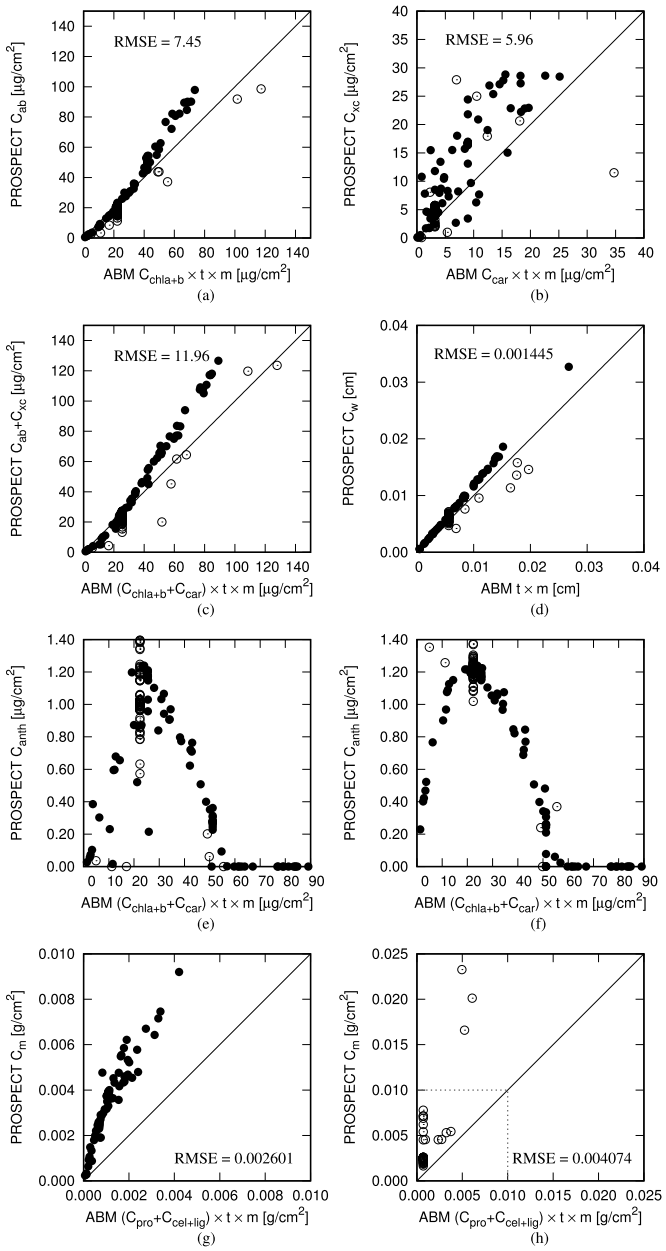

Fig. 4. Correlation of parameters in PROSPECT-D and ABM-B (listed). (a) C_{ab} versus $C_{chla+b} \times t \times m$. (b) C_{xc} versus $C_{car} \times t \times m$. (c) $C_{ab} + C_{xc}$ versus $(C_{chla+b} + C_{car}) \times t \times m$. (d) C_w versus $t \times m$. (e) and (f) C_{anth} versus $(C_{chla+b} + C_{car}) \times t \times m$. (g) and (h) C_m versus $(C_{pro} + C_{cel+lig}) \times t \times m$, dotted lined box represents range from (g) (• $CCR_{constant}$, ○ $CCR_{varying}$).

inverse direction, the model takes leaf spectra and estimates these seven parameters. The parameters chosen for the ABM-B model and the parameter estimations from a single PROSPECT-D inversion (including all pigments) were correlated for all 150 spectra as shown in Fig. 4 for C_{ab}, C_{xc}, C_{anth}, C_w, and C_m. These data were subdivided into two categories: the $CCR_{constant}$ set that used default values for δ_e, δ_p, δ_s, δ_c, and θ (5, 1, 5, 1, 0) and included sieve effects (filled circles in figures), and the $CCR_{varying}$ set that varied all or some of these parameters (unfilled circles in figures). The majority of outliers in the correlations were associated with the $CCR_{varying}$ parameter sets. PROSPECT-D parameter estimates from a single initial condition where all pigments were included are shown. Although spectral differences were noted in Fig. 3, there was no statistically significant difference in pigment estimates between inversions including those that excluded C_{br} or C_{anth} for the results shown in Fig. 4. An exception to this is the anthocyanin concentration; the distribution of the C_{anth} estimates is altered when brown pigments are excluded.

Fig. 4(a) shows the correlations between C_{ab} and $C_{chla+b} \times t \times m$. This correlation graph indicates that the chlorophyll in the two models has good agreement and similar values would model similar looking leaf spectra. The same is not true for C_{xc} in Fig. 4(b). Although there is some correlation between C_{xc} and $C_{car} \times t \times m$, the expected linear trend between the two models is not as pronounced as with C_{ab}. This may be due in part to the specific absorption coefficients used for chlorophyll and carotenoids. PROSPECT-D uses separate empirically calibrated spectra for chlorophylls and carotenoids. A comparison of chlorophyll spectra used in modeling is presented in [2] and [6]. ABM-B uses the chlorophyll SAC that would have included some carotenoid absorption as discussed in Section I. The SAC for the carotenoids is taken from an alternate source [23]. Fig. 4(b) indicates that PROSPECT-D is estimating a higher level of carotenoids than was specified for ABM-B in most samples. It is hypothesized that PROSPECT-D registers a combination of explicitly specified and implicitly included carotenoids in ABM-B. An increase in pigment concentration of the same magnitude would be less prominent (would generate a smaller percentage offset) in the C_{ab} graph than the C_{xc} graph as C_{ab} has a higher concentration in the majority of samples. By combining the chlorophyll and carotenoid content in both models, a stronger correlation was found between these pigments than for the carotenoid case alone [Fig. 4(c)]. This figure shows the $(C_{chla+b} + C_{car}) \times t \times m$ combination from ABM-B as correlated with the $C_{ab} + C_{xc}$ combination from PROSPECT-D. The average RMSE value (in μg/cm^2) is 7.45, 5.96, and 11.62 for chlorophyll, carotenoids, and their combination, respectively. These RMSE values are higher than the averages found in Féret *et al.* as compared to actual leaf data (4.23 and 3.39 for chlorophyll and carotenoids, respectively) [6]. For these subfigures, the ABM-B model inputs are always at a slightly lower value that those estimated by PROSPECT-D. Fig. 4(e) and (f) shows correlations found between C_{anth} and $(C_{chla+b} + C_{car}) \times t \times m$ with and without brown pigments, respectively. At low concentrations of chlorophyll and carotenoids, anthocyanin estimates increase with increasing $C_{chla+b} + C_{car}$. However, as the concentration of $C_{chla+b} + C_{car}$ exceeds 20 μg/cm^2, the anthocyanin estimate reaches a peak and then declines. The decreased correlation at higher concentrations arises from saturation effects in the reflectance and transmittance. As the pigment concentrations increase, the reflectance and transmittance will reach a minimum value. At this point, additional anthocyanin would not increase the absorption further. The correlated increase and decrease of anthocyanin with $C_{chla+b} + C_{car}$ is more pronounced in the absence of brown pigments [as shown in (f)] as the absorbing range of these pigments overlaps with the absorbing range of the anthocyanins. In the absence of C_{br}, the anthocaynin pigments are the primary

absorbing component near 550 nm. These results agree with the assessment that the ABM-B chlorophyll SAC includes some anthocyanin absorption.

Correlations for C_{br} were investigated, but no direct relationship was found. The only correlation found between C_{br} and a ABM-B parameter was linked to the sieve effect. When the sieve effect was not simulated, PROSPECT-D estimated a much higher C_{br} concentration. This may be partially due to the overall decrease in reflectance for ABM-B spectra. In these cases, the PROSPECT-D inversion estimates an increased C_{br} concentration, decreasing the reflectance near 800 nm as seen in Fig. 3(c) and (d).

Fig. 4(d) shows the correlation between C_w from PROSPECT-D and $t \times m$ from ABM-B. C_w is described as the equivalent water thickness in the PROSPECT-D model and its correlation with $t \times m$ shows very good agreement. Therefore, the water component in ABM-B is directly related to these leaf structure parameters. Reproducing the spectrum of a desiccated leaf is then out of the scope of the design of ABM-B as these structure parameters are also closely tied to the pigment concentrations. The water absorption spectra used in ABM-B [24], [25] and PROSPECT-D [26]–[28] are also from different sources, but both models use measured as opposed to modeled spectra for this parameter. The water absorption spectra used in the two models have a normalized RMSE of 0.024 between them.

Fig. 4(g) and (h) correlates C_m with $(C_{pro}+C_{cel+lig})\times t \times m$. This correlation was split between two subfigures (separated based on $CCR_{constant}$ and $CCR_{varying}$) as the $CCR_{varying}$ subset contained much higher estimates for C_m than the $CCR_{constant}$ subset. This correlation shows some agreement, but the nonlinearity and deviation from the 1:1 line may indicate a more complex correlation between these similar model parameters. The specific absorption coefficients for ABM-B's C_{pro} and $C_{cel+lig}$ were taken from the original PROSPECT model [14].

Finally, the estimates of the structure parameter, N, were analyzed. Using the $CCR_{constant}$ parameter sets, Fig. 5(a) shows a nonlinear and inverse relationship between N and $t \times m$. This relationship is well described by logarithmic curve resulting in an R^2 value of 0.94. A nonlinear relationship is expected when considering the nature of light absorbance. In PROSPECT-D, the N parameter is used in calculating the absorbance of a single layer of leaf material. It is then used when determining the transmittance and reflectance of each layer in the leaf. In ABM-B, increasing the thickness of the leaf results in increased absorbance and decreased transmittance and reflectance. This does not align directly with the effects of the N parameter as an increase in N results in increased reflectance but decreased transmittance. This may relate to the logarithmic relationship between these parameters as their effects are partially in opposition. Because the parameter concentrations in ABM-B are volume-based and the concentration in PROSPECT-D are area-based, their relationships to these structure parameters differ. Increasing the thickness parameter in ABM-B effectively increases the corresponding area-based concentration.

When the $CCR_{constant}$ and $CCR_{varying}$ sets are both considered, it is clear that the $CCR_{varying}$ parameters also affect N as shown in Fig. 5(b). In this figure, constant $t \times m$ values result in significantly different estimates for N in $CCR_{varying}$ and the trend seen in (a) is no longer obvious. Fig. 5(c) shows the individual effects of δ_e, δ_p, and δ_s. Lower values for these cell-cap ratio parameters correspond to cell caps that are more optically rough and cause more diffusion of the light [7]. Lower values result in a higher estimation for N as the reflectance is increased and transmittance is decreased. The effect of δ_s is much less pronounced than the other two aspect ratios likely due to its situation deeper in the leaf tissue. Similar to the $t \times m$ comparison, the relationship between N and these three parameters is not linear, but is well described by a logarithmic curve with R^2 values of 0.99, 0.98, and 0.96 for δ_s, δ_p, and δ_e, respectively.

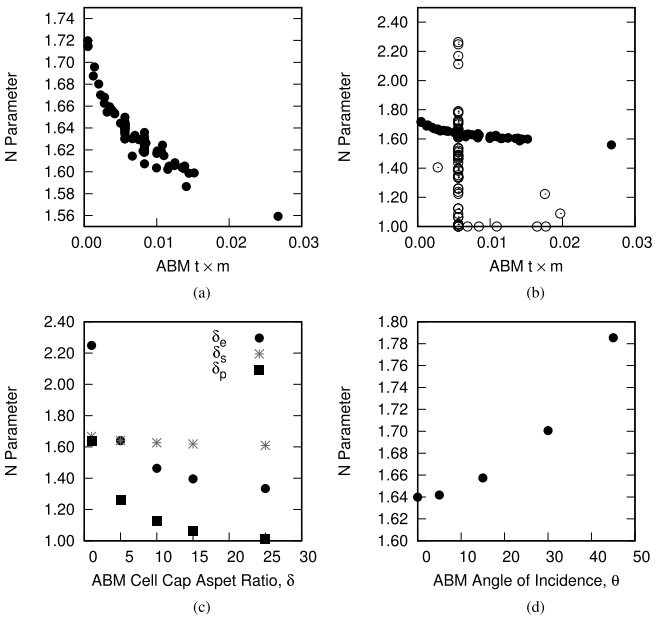

Fig. 5. Changes induced in the N parameter by (a) $t \times m$ (using $CCR_{constant}$), (b) $t \times m$ (using $CCR_{constant}$ and $CCR_{varying}$), (c) δ_e, δ_p, and δ_s, and (d) θ.

The final parameter that has a substantial effect on the N parameter is the angle of incidence (θ) as shown in Fig. 5(d). Increasing the angle of incidence causes N to increase nonlinearly. When θ increases, the reflectance of the leaf increases and the transmittance decreases. At angles close to normal, N is estimated to be smaller as more light is transmitted through the leaf and less is reflected. The increase in reflectance due to the angle of incidence is related to the specular component of reflectance that is produced at large angles to the normal. PROSPECT-D does not have a function to account for variations in angle of incidence or specular reflection so the structure parameter is the only option to account for the changes induced by this ABM-B parameter. The structure parameter in PROSPECT-D is accounting for many parameters in ABM-B and it is very difficult to determine how all of these parameters are combined in the final estimation of N. This parameter in particular has the potential to be expanded to better describe the structure of a leaf in future invertible models. Accounting for angle of incidence separately is one such expansion that has been explored [3], but separating

large-scale and small-scale structure changes and including surface properties as a separate feature may improve the output of an inverted model further.

VI. Conclusion

By comparing the effects of altering each input parameter individually, a wavelength-specific sensitivity was described for selected parameters in both models. A second comparison used spectra generated by ABM-B to estimate parameters through the inversion of PROSPECT-D. Correlations between the input parameters from ABM-B and the estimated parameters from PROSPECT-D were then observed. The chlorophyll and carotenoid estimations from the two models appear to agree in trend, but the PROSPECT-D model tends to estimate these pigments at a higher concentration than is specified in ABM-B in the $\text{CCR}_{\text{constant}}$ parameter sets. The dry matter parameter in PROSPECT-D appears to correlate with the protein, cellulose, and lignin in the ABM-B model but the relationship is not 1:1. The water thickness in PROSPECT-D correlates with the thickness of the leaf and mesophyll percentage in ABM-B. The most complicated correlation drawn between the two models was the relationship between PROSPECT-D's structure parameter (N) and the illumination angle and cellular aspect ratios in ABM-B. N summarizes several leaf structure effects described in ABM-B. A nonlinear correlation can be found when only t, m, and concentration-based parameters are modified, but other structure parameters such as cell cap aspect ratios make the mapping of these relationships more complex. Increasing the cell aspect ratios of the epidermis, palisade, and spongy mesophyll cells decreases the estimation for N as higher values for these parameters result in less diffusion of light. The angle of incidence also has a substantial effect on N and increasing the angle in ABM-B results in an increased estimation of N in PROSPECT-D.

By developing correlations between the parameters in these two models and understanding the effects of individual parameters, informed decisions can be made regarding feature inclusion in a future model. Expanding the parameter list in PROSPECT-D while maintaining efficient invertibility will allow for more information to be estimated nondestructively. Of particular interest in the findings here is the N parameter is combining a number of parameters from the ABM-B model. This allows for fewer parameters in the inversion but may be reducing PROSPECT-D's ability to model leaf thickness and geometry as well as cellular roughness. By separating this structure parameter into two parameters (cell-level and leaf-level), the applications may be expanded. In ABM-B, the cellular aspect ratios have a large effect on the leaf reflectance and transmittance and should be included to some degree in future modeling.

Acknowledgment

The authors would like to thank J.-B. Féret, G. Baranoski, and the anonymous reviewers for their feedback and corrections in usage and descriptions of the PROSPECT-D and AMB-B models.

References

[1] B. Hosgood, S. Jacquemoud, G. Andreoli, J. Verdebout, G. Pedrini, and G. Schmuck, "The JRC leaf optical properties experiment (LOPEX'93)," Eur. Commission Joint Res. Center, Italy, Rome, Inst. Remote Sens. Appl., Tech. Rep. EUR-16096-EN, 1995.

[2] J.-B. Féret *et al.*, "PROSPECT-4 and 5: Advances in the leaf optical properties model separating photosynthetic pigments," *Remote Sens. Environ.*, vol. 112, no. 6, pp. 3030–3043, Jun. 2008.

[3] S. Jay, R. Bendoula, X. Hadoux, J.-B. Féret, and N. Gorretta, "A physically-based model for retrieving foliar biochemistry and leaf orientation using close-range imaging spectroscopy," *Remote Sens. Environ.*, vol. 177, pp. 220–236, May 2016.

[4] G. V. Baranoski, S. Van Leeuwen, and T. F. Chen, "On the decomposition of foliar hyperspectral signatures for the high-fidelity discrimination and monitoring of crops," *Proc. SPIE*, vol. 9880, Apr. 2016, p. 98800G.

[5] G. V. G. Baranoski, S. Van Leeuwen, and T. F. Chen, "In silico analysis of decomposed reflectances of C3 and C4 plants aiming at the effective assessment of crop needs," *J. Appl. Remote Sens.*, vol. 11, no. 2, May 2017, Art. no. 026012.

[6] J.-B. Féret, A. A. Gitelson, S. D. Noble, and S. Jacquemoud, "PROSPECT-D: Towards modeling leaf optical properties through a complete lifecycle," *Remote Sens. Environ.*, vol. 193, pp. 204–215, May 2017.

[7] G. V. Baranoski, "Modeling the interaction of infrared radiation (750 to 2500 nm) with bifacial and unifacial plant leaves," *Remote Sens. Environ.*, vol. 100, no. 3, pp. 335–347, Feb. 2006.

[8] H. W. Gausman, W. A. Allen, and R. Cardenas, "Reflectance of cotton leaves and their structure," *Remote Sens. Environ.*, vol. 1, no. 1, pp. 19–22, Mar. 1969.

[9] S. W. Maier, "Modeling the radiative transfer in leaves in the 300 nm to 2.5 μm wavelength region taking into consideration chlorophyll fluorescence: The leaf model slope," Ph.D. dissertation, Deutsches Zentrum für Luft-und Raumfahrt, Bibliotheks-und Informationswesen, Cologne, Germany, 2000.

[10] S. Jacquemoud and F. Baret, "PROSPECT: A model of leaf optical properties spectra," *Remote Sens. Environ.*, vol. 34, no. 2, pp. 75–91, Nov. 1990.

[11] J. Jiang, A. Comar, P. Burger, P. Bancal, M. Weiss, and F. Baret, "Estimation of leaf traits from reflectance measurements: Comparison between methods based on vegetation indices and several versions of the PROSPECT model," *Plant Methods*, vol. 14, no. 1, p. 23, Dec. 2018.

[12] W. A. Allen, H. W. Gausman, A. J. Richardson, and J. R. Thomas, "Interaction of isotropic light with a compact plant leaf," *J. Opt. Soc. Amer.*, vol. 59, no. 10, pp. 1376–1379, 1969.

[13] G. V. G. Baranoski and D. Eng, "An investigation on sieve and detour effects affecting the interaction of collimated and diffuse infrared radiation (750 to 2500 nm) with plant leaves," *IEEE Trans. Geosci. Remote Sens.*, vol. 45, no. 8, pp. 2593–2599, Aug. 2007.

[14] S. Jacquemoud, S. L. Ustin, J. Verdebout, G. Schmuck, G. Andreoli, and B. Hosgood, "Estimating leaf biochemistry using the PROSPECT leaf optical properties model," *Remote Sens. Environ.*, vol. 56, no. 3, pp. 194–202, Jun. 1996.

[15] S. Jacquemoud, C. Bacour, H. Poilve, and J. P. Frangi, "Comparison of four radiative transfer models to simulate plant canopies reflectance: Direct and inverse mode," *Remote Sens. Environ.*, vol. 74, no. 3, pp. 471–481, Dec. 2000.

[16] S. Jacquemoud and S. Ustin, *Leaf Optical Properties*. Cambridge, U.K.: Cambridge Univ. Press, 2019.

[17] *Run ABM-B Online*, Natural Phenomena Simulation Group, Univ. Waterloo, Waterloo, ON, Canada, 2011. [Online]. Available: http://www.npsg.uwaterloo.ca/models/ABMB.php

[18] D. M. Hamby, "A review of techniques for parameter sensitivity analysis of environmental models," *Environ. Monitor. Assessment*, vol. 32, no. 2, pp. 135–154, Sep. 1994.

[19] L. Northam and G. V. G. Baranoski, "A novel first principles approach for the estimation of the sieve factor of blood samples," *Opt. Express*, vol. 18, no. 7, pp. 7456–7469, Mar. 2010.

[20] C. Proctor, B. Lu, and Y. He, "Determining the absorption coefficients of decay pigments in decomposing monocots," *Remote Sens. Environ.*, vol. 199, pp. 137–153, Sep. 2017.

[21] T. Fourty, F. Baret, S. Jacquemoud, G. Schmuck, and J. Verdebout, "Leaf optical properties with explicit description of its biochemical composition: Direct and inverse problems," *Remote Sens. Environ.*, vol. 56, no. 2, pp. 104–117, May 1996.
[22] F. Baret and T. Fourty, "Estimation of leaf water content and specific leaf weight from reflectance and transmittance measurements," *Agronomie*, vol. 17, nos. 9–10, pp. 455–464, 1997.
[23] D. Eng and G. V. G. Baranoski, "The application of photoacoustic absorption spectral data to the modeling of leaf optical properties in the visible range," *IEEE Trans. Geosci. Remote Sens.*, vol. 45, no. 12, pp. 4077–4086, Dec. 2007.
[24] R. M. Pope and E. S. Fry, "Absorption spectrum (380–700 nm) of pure water. II. Integrating cavity measurements," *Appl. Opt.*, vol. 36, no. 33, pp. 8710–8723, 1997.
[25] K. F. Palmer and D. Williams, "Optical properties of water in the near infrared," *J. Opt. Soc. Amer.*, vol. 64, no. 8, pp. 1107–1110, 1974.
[26] H. Buiteveld, J. H. M. Hakvoort, and M. Donze, "Optical properties of pure water," *Proc. SPIE*, vol. 2258, Oct. 1994, pp. 174–184.
[27] L. Kou, D. Labrie, and P. Chylek, "Refractive indices of water and ice in the 0.65-to 2.5-μm spectral range," *Appl. Opt.*, vol. 32, no. 19, pp. 3531–3540, 1993.
[28] D. M. Wieliczka, S. Weng, and M. R. Querry, "Wedge shaped cell for highly absorbent liquids: Infrared optical constants of water," *Appl. Opt.*, vol. 28, no. 9, p. 1714, May 1989.

Reisha D. Peters received the B.Sc. and M.Sc. degrees from the University of Saskatchewan, Saskatoon, SK, Canada, in 2013 and 2016, respectively, where she is pursuing the Ph.D. degree in biological engineering.

Her research interests include spectroscopic analysis and computer modeling for simple, fast analysis of samples in a variety of settings and disciplines.

Scott D. Noble received the B.Sc. degree from the University of Guelph, Guelph, ON, Canada, in 1999, the M.Sc. degree from the University of Saskatchewan, Saskatoon, SK, Canada, in 2002, and the Ph.D. degree from the University of Guelph, in 2007.

He is an Associate Professor with the Department of Mechanical Engineering, University of Saskatchewan. His research activities include studies on pneumatic conveying in agricultural machinery, leaf optical property modeling, and applications of imaging and spectroscopy in mining, nondestructive testing, and plant phenotyping.